ORIGINAL ARTICLE

UDC: 617.736-08:617.751
https://doi.org/10.2298/VSP150709149R

Correlation between visual acuity, external limiting membrane and photoreceptor status in patients with neovascular age-related macular degeneration treated with bevacizumab

Korelacija između vidne oštrine, spoljašnje granične membrane i fotoreceptora kod bolesnika sa neovaskularnom senilnom degeneracijom žute mrlje lečenih bevacizumabom

Dragana Ristić*†, Miroslav Vukosavljević*†, Marko Kontić*†, Petar Ristić*‡, Dubravko Bokonjić*§, Mirjana Janićijević-Petrović‖¶, Antoaneta Adžić Zečević††, Katarina Janićijević‖¶**

University of Defence, *Faculty of Medicine of the Military Medical Academy, Belgrade, Serbia; Military Medical Academy, †Clinic for Ophthalmology, ‡Endocrinology Clinic, §National Poison Control Centre, Belgrade, Serbia; Clinical Centre Kragujevac, ‖Clinic for Ophthalmology, Kragujevac, Serbia; University of Kragujevac, ¶Faculty of Medical Sciences, Kragujevac, Serbia; Clinical Centre of Montenegro, **Clinic for Ophthalmology, Podgorica, Montenegro; University of Montenegro, ††Faculty of Medicine, Podgorica, Montenegro

Abstract

Background/Aim. The integrity of outer retinal structures, primarily the photoreceptor layer, is important because of its direct correlation with visual acuity. The aim of this study was to investigate the correlation between best-corrected visual acuity (BCVA), the foveal photoreceptor-inner segment/outer segment (IS/OS) junction and external limiting membrane (ELM) in patients with neovascular age-related macular degeneration (NVAMD) after the treatment with bevacizumab, as well as the correlation between the above-mentioned parameters and different types of neovascular membrane, classified by fluorescein angiography (FA). **Methods.** The study included 82 patients with NVAMD, treated with intravitreal bevacizumab. All patients underwent a basic ophthalmological examination, FA and optical coherence tomography (OCT). Based on the results of FA, all the patients were divided into two main groups – type I (the occult and minimally classic) and type II (classic and predominantly classic) of the choroidal neovascular membrane (CNV). The OCT images revealed either the presence or the absence of IS/OS and ELM. **Results.** After the treatment, the mean best corrected visual acuity improved significantly in both groups ($p < 0.01$). Preserved IS/OS and ELM were registered in a smaller number of patients as compared to the condition before the treatment ($p < 0.01$). After the treatment, the mean BCVA was significantly better in patients with preserved IS/OS and ELM ($p < 0.01$). In addition, we registered a higher number of patients with preserved ELM in the first group than in the second group ($p < 0.01$), whereas there was no significant difference in the integrity of IS/OS between the groups ($p > 0.05$). **Conclusion.** The patients with preserved IS/OS and ELM achieved better final visual acuity as compared to the patients without preserved IS/OS and ELM. In our patients, the absence of IS/OS and ELM were more frequent in type II (classic and predominantly classic) CNV than in type I (the occult and minimally classic) CNV.

Key words:
retina; macular degeneration; neovascularization, pathologic; bevacizumab; tomography, optical coherence; fluorescein angiography.

Apstrakt

Uvod/Cilj. Integritet spoljašnjih struktura mrežnjače, primarno sloja fotoreceptora, važan je zbog njihove direktne povezanosti sa oštrinom vida. Cilj rada bio je da se ispita povezanost između najbolje korigovane vidne oštrine, fovealnih fotoreceptora i spoljašnje granične membrane kod bolesnika sa neovaskularnom senilnom degeneracijom žute mrlje nakon lečenja bevacizumabom, kao i odnos navedenih parametara sa različitim tipovima neovaskularne membrane klasifikovane metodom fluoresceinske angiografije. **Metode.** Istraživanjem su obuhvaćena 82 bolesnika sa neovaskular-

Correspondence to: Dragana Ristić, Military Medical Academy, Clinic for Ophtalmology, Crnotravska 17, 11 000 Belgrade, Serbia. Phone: +381 11 233 5090. E-mail: dadana25@yahoo.com

nom senilnom degeneracijom žute mrlje lečena intravitealnom primenom bevacizumaba. Svim ispitanicima urađen je osnovni oftalmološki pregled, fluoresceinska angiografija i optička koherentna tomografija. Na osnovu nalaza fluoresceinske angiografije svi bolesnici podeljeni su u dve osnovne grupe, tip I (okultna i minimalno klasična) i tip II (klasična i predominantno klasična) horoidalne neovaskularne membrane. Pomoću optičke koherentne tomografije defisano je prisustvo ili odsustvo fotoreceptora i spoljašnje granične membrane. **Rezultati.** Prosečna najbolje korigovana vidna oštrina značajno se popravila po završetku lečenja u obe grupe ($p < 0,01$). Očuvan kontinuitet fotoreceptora i spoljašnje granične membrane registrovan je kod manjeg broja ispitanika u odnosu na stanje pre tretmana ($p < 0,01$). Prosečna najbolje korigovana vidna oštrina po završetku lečenja bila je značajno bolja kod ispitanika sa očuvanim fotoreceptorima i spoljašnjom graničnom membranom ($p < 0,01$). Takođe, registrovali smo više ispitanika sa očuvanim kontinuitetom spoljašnje granične membrane u prvoj u odnosu na drugu grupu ($p < 0,01$), dok se broj ispitanika sa očuvanim kontinuitetom fotoreceptora po završetku lečenja nije značajno razlikovao između grupa ($p > 0,05$). **Zaključak.** Kod bolesnika sa očuvanim fotoreceptorima i spoljašnjom graničnom membranom vidna oštrina nakon završetka lečenja bila je značajno bolja u odnosu na ispitanike kod kojih ove strukture nisu bile prisutne. Kod naših ispitanika odsustvo fotoreceptora i spoljašnje granične membrane bilo je češće kod tipa II (klasična i predominantno klasična) u odnosu na tip I (okultna i minimalno klasična) neovaskularne membrane.

Ključne reči:
retina; žuta mrlja, degeneracija; neovaskularizacija, patološka; bevacizumab; tomografija, optička, koherentna; angiografija, fluoresceinska.

Introduction

Choroidal neovascular membrane (CNV) is the main cause of severe visual impairment in patients with wet age-related macular degeneration (AMD). Vascular endothelial growth factor (VEGF) is one of the main factors responsible for the development of CNV. The drugs that block its activity, anti-VEGF drugs, have improved considerably the course of this disease and the patients' quality of life [1–3]. Today, they represent standard therapy for the treatment of neovascular AMD (NVAMD) [4, 5].

Bevacizumab (trade name Avastin®) is a monoclonal VEGF antibody, approved for intravenous use in the management of colorectal carcinoma. In ophthalmology, it is used off-label. The first papers related to the intravitreal administration of this drug in the treatment of NVAMD were published as early as in 2006 [6–8].

Optical coherence tomography (OCT) is a useful tool in the diagnosis and monitoring of AMD. After the introduction of a spectral-domain OCT (SD-OCT), which provides image resolution of up to 5 μm, it becomes possible to see clearly all retinal structures [9, 10]. The monitoring of CNV [presence of intraretinal fluid, subretinal fluid or fluid under the retinal pigment epithelium (RPE)] is important for the assessment of its activity. After the treatment, i.e. after the fluid has retreated, a subretinal fibrosis or atrophy can occur, which consequently influences the status of inner segment/outer segment (IS/OS) and external limiting membrane [11].

The monitoring of the integrity of external retinal layers, primarily the photoreceptor layer, is important because of its direct correlation with visual acuity [12–15]. In some studies, the IS/OS line on the SD-OCT images was reportedly a good indicator for predicting best-corrected visual acuity (BCVA) in NVAMD patients treated with anti-VEGF therapy [16]. ELM status is another useful parameter during the evaluation of retinal morphology and function in patients with NVAMD [17].

The aim of this study was to investigate the correlation between BCVA, IS/OS and ELM in patients with NVAMD after the treatment with bevacizumab, as well as the correlation between the above-mentioned parameters and different types of neovascular membrane, classified by fluorescein angiography (FA).

Methods

This clinical, cohort, prospective, non-randomized study was conducted at the Military Medical Academy, Belgrade, Serbia between February 2013 and February 2015. The protocol of this study was approved by the Ethical Committee of the Military Medical Academy. The patients were informed about the off-label use of bevacizumab.

The study involved 105 patients in total. Out of that number, 23 patients were excluded due to insufficient documentation. Here we present 82 patients, in whom the fluid retreated after the sixth dose of the medication, i.e. the CNV activity decreased. CNV was considered active if contrast leakage was seen on FA and if OCT detected an increased and/or persistent presence of macular fluid. As there is no precise dosing protocol for this medication, based on our experience and after consulting literature, we opted for six-monthly doses.

All patients were over the age of 65 and were suffering from AMD-related subfoveolar CNV which had not been treated previously. To qualify for the study, the patients had to have the mean BCVA of 0.05 or higher (Snellen chart). The patients did not have acute or chronic eye inflammations, other fundus changes or decompensated glaucoma. The presence of early-stage/cataract or pseudophakia were not a reason for the exclusion from the study.

At the beginning, each patient underwent the following: complete ophthalmological examination, BCVA assessment, FA on Topcon Trc-NW7SF fundus camera and OCT on Topcon 1000-SD OCTTOp 1000-T3D3. Based on the FA results, the patients were divided into two main groups, depending on whether they had Type I CNV (the occult and minimally classic) or Type II CNV (classic and predominantly classic) membrane. Each group consisted of

41 patients. Using OCT scans we detected the presence or the absence of ELM and IS/OS. This analysis was conducted by two ophthalmologists independently and in the case of inconsistencies in the findings, it was supervised by the mentor. Structural changes of CNV seen on OCT were analyzed in the subfoveal area of 1 mm. The OCT findings were analyzed immediately before the administration of each dose of the medication. In cases where macular fluid disappeared completely before the sixth dose of the medication was given, we interrupted the treatment and such patients were excluded from the study.

All the patients received 1.25 mg of bevacizumab (0.05 mL of the commercial phial of Avastin®) intravitreally. The control assessments were carried out on the first, seventh and thirtieth days following the intervention. One month after administration of the first dose, the next dose was administered. A total of six doses were administered in one-month intervals (+-2).

Statistical analysis was performed before and after the therapy, using SPSS version 19.0 (SPSS., Chicago, IL, USA).

Distribution of variables was assessed by Kolmogorov-Smirnov test and it was concluded that BCVA-related data should be analyzed using non-parametric statistics. The values within a group were analyzed by Friedman's test. For the comparison of BCVAs between the groups, we used the Mann-Whitney U-test.

Results

The patients [82 patients (eyes), 41 in each group] were between 65 and 92 years old. The average age was 77.2 years in the first group and 77.8 years in the second, one. The mean initial BCVA was 0.19 in the first group, and 0.14 in the second one. After the therapy, the mean BCVA was 0.42 in the first, and 0.30 in the second group ($p < 0.01$) (Table 1).

Before the therapy, preserved ELM was registered in all patients (100%), in both groups. In the first group, after the sixth dose, ELM was preserved in 26 patients (63.4%) and in the second one in 11 (26.8%) patients. Before the treatment, the IS/OS was preserved in 39 (95.2%) patients from the first group, and in 35 (85.4%) patients in the second group. After the treatment, the number of patients with preserved IS/OS in the first group decreased to 28 (68.3%) and to 22 (53.4%) in the second group (Tables 2).

In the first group, in patients in whom ELM was preserved, the mean BCVA was 0.19. After the treatment, ELM was preserved in 26 patients and their mean BCVA was 0.53 ($p < 0.01$). After the treatment, in 15 patients in whom ELM was not preserved, the mean BCVA was 0.23 (0.19–0.23) ($p < 0.05$). In the first group, IS/OS were preserved in 39 patients before the treatment, and their mean BCVA was 0.15. After the treatment, IS/OS was preserved in 28 patients, with mean BCVA of 0.39 ($p < 0.01$). In two patients without preserved IS/OS before the therapy the mean BCVA was 0.10, and after the therapy, IS/OS were absent in 13 patients with mean BCVA 0.18 ($p > 0.05$) (Table 3).

In the second group, in patients in whom ELM was preserved, the mean BCVA was 0.14. After the treatment, ELM was preserved in 11 patients and their mean BCVA was 0.46 ($p < 0.01$). In 30 patients in whom ELM was not preserved, after the treatment the mean BCVA was 0.24 ($p < 0.05$). In the second group, 35 patients had complete IS/OS before the treatment, and their mean BCVA was 0.22. After the treatment, IS/OS were preserved in 22 patients, with mean BCVA of 0.33 ($p < 0.05$). In six patients without preserved IS/OS before the therapy the mean BCVA was 0.15, and after the therapy IS/OS were absent in 19 patients with mean BCVA 0.22 ($p < 0.05$) (Table 3).

Table 1

Best-corrected visual acuity (BCVA) before and after the administration of bevacizumab

Group	BCVA		*p*-value
	pre-treatment	post-treatment	
I	0.19	0.42	< 0.01
II	0.14	0.30	

Group I – occult and minimally classic membrane; Group II – classic and predominantly classic membrane.

Table 2

Integrity of external limiting membrane (ELM) and inner segment/outer segment (IS/OS) in bevacizumab-treated patients according to groups

Parameter	Group I, n (%)		Group II, n (%)	
	pre-treatment	post-treatment	pre-treatment	post-treatment
ELM				
present	41 (100)	26 (63.4)	41 (100)	11 (26.8)
absent	–	15 (36.5)	–	30 (73.2)
IS/OS				
present	39 (95.2)	28 (68.3)	35 (85.4)	22 (53.4)
absent	2 (4.9)	13 (31.7)	6 (14.6)	19 (46.6)

Group I – occult and minimally classic membrane; Group II – classic and predominantly classic membrane.

Table 3
Best-corrected visual acuity (BCVA) according to external limiting membrane (ELM) and inner segment/outer segment (IS/OS) in the group I and the group II

Groups	BCVA	
	pre-treatment	post-treatment
Group I		
ELM		
present	0.19	0.53
absent	/	0.23
IS/OS		
present	0.15	0.39
absent	0.10	0.18
Group II		
ELM		
present	0.14	0.46
absent	/	0.24
IS/OS		
present	0.22	0.33
absent	0.15	0.22

Group I – occult and minimally classic membrane;
Group II – classic and predominantly classic membrane.

The results of our study showed that after the treatment there were 26 patients with preserved ELM in the first group (the occult and minimally classic CNV), as compared to 11 patients in the second group (classic and predominantly classic) ($p < 0.01$). After the treatment, IS/OS were preserved in 28 patients in the first group and in 22 patients in the second group ($p > 0.05$) (Table 1).

Discussion

The results of our study confirmed that the visual acuity in patients with wet AMD was significantly improved after the intravitreal administration of bevacizumab, as previous studies had demonstrated [1–3, 6–8].

There are several types of anti-VEGF medications, registered for intravitreal administration. Since the study by Martin al. [3] CATT showed that ranibizumab is not superior to bevacizumab in terms of their effects, and, as bevacizumab is significantly cheaper, we decided to use bevacizumab.

The protocol for the administration of anti-VEGF drugs has not been precisely established yet. In the studies such as ones by Brown et al. [1] (ANCHOR) and Rosenfeld et al. [2] (Marina), this medication was administered monthly. Some studies dealt with treat-and-extend dosing regimens, whereas in other studies, the dosing regimen was *pro re nata* (PRN) – treat and observe [5]. Based on our previous experience, we decided to apply a monthly dosing regimen.

The correlation between the type of neovascular membrane (identified by FA), and its structural characteristics (identified by OCT) was described by Freund et al [18]. The final visual acuity in patients with NVAMD is influenced by various changes in the macula (subretinal, intraretinal or fluid under the RPE) [11, 19]. The drug itself has no effect either on ELM or on IS/OS, but after the treatment is over, and after the fluid retreats, the integrity of these parameters influences the final visual acuity, which was described by many authors [14, 15, 20].

A correlation between visual acuity, ELM and IS/OS integrity in the treatment of neovascular AMD with photodynamic therapy was described as early as in 2010 by Oishi et al. [15], and was also mentioned by Sayanagi et al. [16], but subsequent to anti-VEGF therapy. The importance of these structures in the preservation of vision in patients with uveitic macular oedema was described by Tortorela et al. [14].

Sayanagi et al. [16] confirm the importance of IS/OS status in patients who were given anti-VEGF therapy and conclude that IS/OS is a good indicator in terms of prognosis for visual acuity following an anti-VEGF therapy.

Shin et al. [20] conclude that the integrity of foveal photoreceptors is strongly correlated with final visual acuity after the treatment in patients with NVAMD.

Kwon et al. [13] conclude that IS/OS and ELM can be good predictors of visual acuity after anti-VEGF therapy.

Upon the analysis of our data, we noted that the presence of ELM and IS/OS correlate with better visual acuity, both before and after the therapy. A significant role of ELM and IS/OS, as important prognostic factors for final BCVA, was also confirmed by Mathew et al [19].

Our study showed the significant improvement of BCVA in patients with preserved ELM and IS/OS in both groups, whereas in patients with not preserved ELM and IS/OS, the BCVA was lower (there was an improvement, but the difference was not statistically significant).

The number of patients with preserved IS/OS and ELM decreased after the treatment, especially in the second group, where the number of patients with preserved ELM after the therapy was considerably lower. This means that there were more patients with preserved ELM and IS/OS in the first group (the occult and minimally classic CNV) than in the second group (classic and predominantly classic CNV). The literature offers diverse findings regarding this issue. Bloch et al. [21] in their study obtained the findings similar to ours, while Freund et al. [18] in their study actually argue that the response to anti-VEGF therapy is better in patients from the second group (classic and predominantly classic CNV).

The studies, such as ANCHOR [1] and MARINA [2], showed that, regardless of the type of neovascular membra-

ne, classified by FA method, the vision would improve after the anti-VEGF therapy. We confirmed such findings, as well as that visual acuity is considerably better if IS/OS and ELM are preserved at the end of the treatment.

Conclusion

The presence of ELM and IS/OS is an important prognostic factor for final visual acuity in patients with NVAMD. The absence of ELM and IS/OS is more frequent in type II CNV (classic and predominantly classic) than in type I CNV (the occult and minimally classic) and this is the reason why these patients can be expected to have somewhat lower final visual acuity after the anti-VEGF therapy.

The development of modern technology provides an even more precise insight into the structure of the neovascular membrane, so future analyses will be able to define even more precisely its various structural parameters and open new approaches to treating these patients.

REFERENCES

1. *Brown DM, Michels M, Kaiser PK, Heier JS, Sy JP, Ianchulev T.* ANCHOR Study Group. Ranibizumab versus verteporfin photodynamic therapy for neovascular age-related macular degeneration: Two-year results of the ANCHOR study. Ophthalmology 2009; 116(1): e57−65.
2. *Rosenfeld PJ, Brown DM, Heier JS, Boyer DS, Kaiser PK, Chung CY.* MARINA Study Group. Ranibizumab for neovascular age-related macular degeneration. N Eng J Med 2006; 355(14): 1419−31.
3. *Martin DF, Maguire MG, Fine SL, Ying GS, Jaffe GJ, Grunwald JE*, et al. Comparison of Age-related Macular Degeneration Treatments Trials (CATT) Research Group. Ranibizumab and bevacizumab for treatment of neovascular age-related macular degeneration: two-year results. Ophthalmology 2012; 119(7): 1388−98.
4. *American Academy of Ophthalmology.* Age-related macular degeneration. Prefferd practice pattern guideline. San Francisco, CA: American Academy of Ophthalmology; 2014.
5. *Agarwal A, Rhoades WR, Hanout M, Soliman MK, Sarwar S, Sadiq MA*, et al. Management of neovascular age-related macular degeneration: Current state-of-the-art care for optimizing visual outcomes and therapies in development. Clin Ophthalmol 2015; 9: 1001−15.
6. *Rosenfeld PJ, Moshfeghi AA, Puliafito CA.* Optical coherence tomography findings after an intravitreal injection of bevacizumab (avastin) for neovascular age-related macular degeneration. Ophthalmic Surg Lasers Imaging 2005; 36(4): 331−5.
7. *Avery RL, Pieramici DJ, Rabena MD, Castellarin AA, Nasir MA, Giust MJ.* Intravitreal bevacizumab (Avastin) for age-related macular degeneration. Ophthalmology 2006; 113: 363−72. e5.
8. *Bashshur ZF, Bazarbachi A, Schakal A, Haddad ZA, El Haibi CP, Noureddin BN.* Intravitreal bevacizumab for the management of choroidal neovascularization in age-related macular degeneration. Am J Ophthalmol 2006; 142(1): 1−9.
9. *Keane PA, Liakopoulos S, Chang KT, Wang M, Dustin L, Walsh AC,* et al. Relationship between optical coherence tomography retinal parameters and visual acuity in neovascular age-related macular degeneration. Ophthalmology 2008; 115(12): 2206−14.
10. *Kashani AH, Keane PA, Dustin L, Walsh AC, Sadda SR.* Quantitative subanalysis of cystoid spaces and outer nuclear layer using optical coherence tomography in age-related macular degeneration. Invest Ophthalmol Vis Sci 2009; 50(7): 3366−73.
11. *Jaffe GJ, Martin DF, Toth CA, Daniel E, Maguire MG, Ying GS,* et al. Comparison of age-related macular degeneration treatments trials research group. Macular morphology and visual acuity in the comparison of age-related macular degeneration treatments trials. Ophthalmology 2013; 120(9): 1860−70.
12. *Wong IY, Iu LP, Koizumi H, Lai WW.* The inner segment/outer segment junction: What have we learnt so far? Curr Opin Ophthalmol 2012; 23(3): 210−8.
13. *Kwon YH, Lee DK, Kim HE, Kwon O*W. Predictive findings of visual outcome in spectral domain optical coherence tomography after ranibizumab treatment in age-related macular degeneration. Korean J Ophthalmol 2014; 28(5): 386−92.
14. *Tortotella P, Ambrosio E, Iannetti L, de Marco F, la Cava M.* Correlation betwen visual acuity, inner segment/outer segment junction, and cone outer segment tips line integrity in uveitic macular edema. Biomed Res Int 2015: 853728.
15. *Oishi A, Hata M, Shimozono M, Mandai M, Nishida A, Kurimoto Y.* The significance of external limiting membrane status for visual acuity in age-related macular degeneration. Am J Ophthalmol 2010; 150(1): 27−32.e1.
16. *Sayanagi K, Sharma S, Kaiser PK.* Photoreceptor status after antivascular endothelial growth factor therapy in exudative age-related macular degeneration. Br J Ophthalmol 2009; 93(5): 622−6.
17. *Hagan MJ, Alvarado JA, Weddell JE.* Histology of the human eye: an atlas and textbook. Philadelphia: Saunders; 1971. p. 393−522.
18. *Freund KB, Zweifel SA, Retina EM.* Do we need a new classification for choroidal neovascularization in age-related macular degeneration? Retina 2010; 30(9): 1333−49.
19. *Mathew R, Richardson M, Sivaprasad S.* Predictive value of spectral-domain optical coherence tomography features in assessment of visual prognosis in eyes with neovascular age-related macular degeneration treated with ranibizumab. Am J Ophthalmology 2013; 155(4): 720−6, 726.e1.
20. *Shin HJ, Chung H, Kim HC.* Association between foveal microstructure and visual outcome in age-related macular degeneration. Retina 2011; 31(8): 1627−36.
21. *Bloch SB, Lund-Andersen H, Sander B, Larsen M.* Subfoveal fibrosis in eyes with neovascular age-related macular degeneration treated with intravitreal ranibizumab. Am J Ophthalmol 2013; 156(1): 116−24.

Received on July 9, 2015.
Revised on March 10, 2016.
Accepted on May 18, 2016.
Online First June, 2016.

ORIGINAL ARTICLE

UDC:613.168::616.2]:[537.531::616.432-053.2
https://doi.org/10.2298/VSP151130279S

Calculation of electromagnetic field from mobile phone induced in the pituitary gland of children head model

Izračunavanje elektromagnetnog polja mobilnog telefona unutar hipofize na modelu glave deteta

Vladimir Stanković*, Dejan Jovanović*, Dejan Krstić*, Vera Marković†, Momir Dunjić‡

University of Niš, *Faculty of Occupational Safety, †Faculty of Electronic Engineering, Niš, Serbia; University of Priština, ‡Faculty of Medicine, Kosovska Mitrovica, Serbia

Abstract

Background/Aim. A mobile phone is a source of electromagnetic radiation located close to the head and consequently its intense use may cause harmful effects particularly in younger population. The aim of this study was to investigate the influence of electromagnetic field of the mobile phone on the pituitary gland of the child. **Methods**. In order to obtain the more accurate results for this research 3D realistic model of child's head whose size corresponds to an average child (7 years old) was created. Electric field distribution in child head model and values of Specific Absorption Rate (SAR) at the region of pituitary gland were determined. This study was performed for the frequencies of 900 MHz, 1800 MHz, and 2100 MHz, as the most commonly used in mobile communications. The special attention was dedicated to the values of the electric field and the values of the SAR in the pituitary gland. For all frequencies over 10 g and 1 g of tissue average SAR was calculated. The electric field distribution and values of average SAR for 10 g and 1 g trough the model of child's head were obtained by the using numerical calculation based on the Finite Integration Technique (FIT). **Results**. The largest value of electric field in the region of the pituitary gland was at the frequency of 900 MHz, as a consequence of the highest penetration depth. Lower values of the electric field in the region of the pituitary gland were at frequencies of 1,800 MHz and 2,100 MHz. The SAR in the pituitary gland decreased as the frequency increased as a direct consequence of lower penetration depth. **Conclusion**. The electric field strength from a mobile phone is higher than the value specified by standards for the maximum allowable exposure limits. The high values of the electric field are not only in the vicinity of a mobile phone but also in tissues and organs of the human head. Particular attention should be paid to the exposure of children to radiation of mobile phones. Smaller dimensions of children's head and smaller thickness of tissues and organs have as a consequence greater penetration of electromagnetic waves.

Key words:
cellular phone; electromagnetic fields; child; models, theoretical; pituitary hormones.

Apstrakt

Uvod/Cilj. Mobilni telefon je izvor elektromagnetnog zračenja u blizini glave i zbog toga njegova preterana upotreba može prouzrokovati štetne efekte osobito kod mlađe populacije. Cilj ovog rada bio je da istraži uticaj električnog polja mobilnog telefona kao izvora elektromagnetnog zračenja na hipofizu deteta. **Metode**. U cilju dobijanja što tačnijih rezultata napravljen je realan 3D model glave deteta čije dimenzije odgovaraju dimenzijama deteta od 7 godina. Određena je raspodela električnog polja unutar modela glave deteta i vrednosti specifične količine apsorbovane energije *Specific Absorption Rate* (SAR) u predelu hipofize. Ovo istraživanje izvršeno je za frekvencije od 900 MHz, 1 800 MHz i 2 100 MHz kao najčešće korišćene frekvencije u mobilnom komunikacionom sistemu. Posebna pažnja bila je posvećena vrednosti električnog polja i vrednosti SAR u hipofizi. Za sve pomenute frekvencije proračunat je usrednjeni SAR za 10 g i 1 g tkiva. Raspodela električnog polja i vrednosti usrednjenog SAR za 10 g i 1 g dobijene su korišćenjem numeričkog metoda koji je zasnovan na tehnici konačnih integrala (FIT). **Rezultati**. Najveća vrednost električnog polja u hipofizi bila je na frekvenciji od 900 MHz zbog veće dubine prodiranja. Za frekvencije od 1 800 MHz i 2 100 MHz vrednosti električnog polja u hipofizi bile su manje. Vrednosti SAR u hipofizi su se smanjivale kako je frekvencija rasla što je direktna posledica manje dubine prodiranja. **Zaključak**. Vrednosti električnog polja koje su posledica zračenja mobilnog telefona veće su od maksimalnih graničnih vrednosti koje su propisane standardima. Velike vrednosti električnog polja nisu samo u okolini telefona, već i u organima i tkivima ljudske glave. Posebnu pažnju treba obratiti na izlaganje dece zračenju mobilnih telefona. Manje dimenzije dečije glave kao i manja debljina tkiva i organa za posledicu ima veću dubinu prodiranja elektromagnetnih talasa.

Ključne reči:
mobilni telefon; elektromagnetna polja; deca; modeli, teorijski; hipofiza, hormoni.

Correspondence to: Vladimir Stanković, University of Niš, Faculty of Occupational Safety, 18 000 Niš, Serbia.
E-mail: vladimir.stankovic@znrfak.ni.ac.rs

Introduction

The wide variety of available options of mobile phones such as games, the internet, calls and video calls, as well as their accessible prices, have led to the daily use of mobile phones mostly in the younger population (children) which can be measured in hours. The mobile phone is a source of electromagnetic radiation which is located close to the head and because of that, the intense use of mobile phones in the younger population causes concern for health effects.

The influence of electromagnetic field from a source of electromagnetic radiation such as mobile phone close to child's head is bigger than an influence on the adult head. This is due to smaller dimension of child's head and consequently thinner pinnae and skulls. Because of that in the case of child's head, the source of electromagnetic radiation is closer to the brain and pituitary gland than in the case of adults head. Relevant data show that the exposure of children to electromagnetic radiation is higher than adult exposure [1, 2].

Because of ethical considerations, human exposure to electromagnetic fields in experimental purposes is limited. Due to this, it is much more convenient to develop a realistic model of the human head by using numerical simulation [3]. Numerical analyses of the human head exposed to electromagnetic radiation of mobile phones provide useful information about absorbed electromagnetic energy under different conditions of exposure. The International Agency for Research on Cancer (IARC) has classified the radiation of electromagnetic fields in 2B group as possibly carcinogenic to human, based on an increased risk of a malignant type of brain cancer. In this category, there is a limited evidence of carcinogenicity in humans and less than sufficient evidence of carcinogenicity in experimental animals [4].

The most important indicator when considering the health risk as a result of the effect of electromagnetic fields is the Specific Absorption Rate (SAR). SAR is directly dependent on the electromagnetic properties of biological tissues exposed to the effects of electromagnetic waves and can be defined as (Equation 1):

$$\mathrm{SAR} = \frac{\sigma |E|^2}{\rho}$$

where E is the maximum value of the internal electric field, σ is the conductivity of the tissue and ρ is the density of the tissue. Maximum values of SAR which must not exceed, are defined in Regulation of the limits of exposure to non-ionizing radiation, Official Gazette of the Republic of Serbia, no. 36/09. This regulation defines the limits of exposure to non-ionizing radiation, or the basic restrictions and reference boundary levels of the population exposure to electric, magnetic and electromagnetic fields of different frequencies [5].

In this research, the level of electric field strength due to mobile phone and SAR values at the region of pituitary gland were determined.

The pituitary is a small gland which has a diameter of around 1cm and a weight of about 0.5–1 g, and it is located at the base of the brain. Physiologically it can be divided into two parts: the front part called the adenohypophysis and the rear part called neurohypophysis. Adenohypophysis secretes six very important hormones, which have a very significant role in the control of metabolic functions of the whole organism such as prolactin, growth hormone (GH), adrenocorticotropic hormone (ACTH), thyroid-stimulating hormone (TSH), luteinizing hormone (LH), follicle-stimulating hormone (FSH). The main role of rear part or neurohypophysis is to store antidiuretic hormone (ADH) and oxytocin. Hormones from the hypothalamus almost completely regulate the secretion of pituitary hormones which are delivered through the bloodstream to the pituitary gland.

As shown in one study [6], exposure to 900 MHz of global system for mobile communication radio frequency (GSM RF) on pituitary hormone levels in healthy males such as: TSH, GH, prolactin and ACTA, led to significant decreases of concentrations of GH and cortisol for about 28% and 12%, respectively.

Due to a higher level of electromagnetic radiation within the child's head compared to that found inside adult's head, the electric field can be one of the causes of serious biological effects on the pituitary gland. Because of harmful effect previously mentioned on the pituitary gland and consequently on the concentration of GH which is essential for normal growth of the child, in this paper special attention is devoted to numerical calculation and distribution of electrical field and SAR in the region of this gland for 7-years old child. Also in this study, an overview of the possible biological effects that may occur in pituitary gland due to exposure to electromagnetic fields is presented.

Methods

In order to obtain more accurate results for this research 3D realistic model of child's head whose size corresponds to an average child (7 years old) had to be created [7, 8]. This model of child's head consisted of following tissues and organs: skin, fat, muscle, skull, jaw with teeth, tongue, eyes, vertebrae, cartilage, spinal cord, cerebrospinal fluid, brain, and pituitary gland.

All of these tissues and organs had to be described by adequate electromagnetic parameters such as electric conductivity, permittivity, heat capacity, density and thermal conductivity [9]. These electromagnetic characteristics vary with frequency and their values for frequencies of 900 MHz, 1,800 MHz, and 2,100 MHz), as the most often used in mobile communication, are shown in Table 1.

Modeling of 3D child's head model was performed in two stages. First external look for every tissues and organs was created in 3D Max Studio [10]. The second step was creating a full model with actual tissues and organs and connecting certain electromagnetic properties with corresponding tissues and organs by using software package CST Microwave Studio [11]. The same software was used for simulation of the electromagnetic field and its influence on child's head. Numerical calculation method used in this software was based on the Finite Integration Technique [12].

External look, horizontal and vertical cross-sections of actual tissues and organs are shown in Figures 1 and 2 with organs numbered according to their numbers in Table 1.

Table 1

Average values of electromagnetic properties of tissues and organs at frequencies of 900 MHz, 1,800 MHz and 2,000 MHz

Tissue/Organ	ε_r	σ (S/m)	ρ* (kg/m^3)	Heat* capacity (kJ/kgK)	Thermal conductivity (W/m°C)
1 – Cortical Bones	12.45[a]	0.143[a]	1,908	1.313	0.32
	11.8[b]	0.275[b]	1,908	1.313	0,32
	11.6[c]	0.328[c]	1,908	1.313	0.32
2 – Brain	45.805[a]	0.7665[a]	1,046	3.630	0.51
	46.1[b]	1.710[b]	1,046	3.630	0.51
	45.50[c]	1.880[c]	1,046	3.630	0.51
3 – Cerebrospinal Fluid	68.60[a]	2.410[a]	1,007	4.096	0.57
	67.2[b]	2.920[b]	1,007	4.096	0.57
	66.80[c]	3.150[c]	1,007	4.096	0.57
4 – Fat	11.30[a]	0.109[a]	911	2.348	0.21
	11.0[b]	0.190[b]	911	2.348	0.21
	10.90[c]	0.224[c]	911	2.348	0.21
5 – Cartilage	42.70[a]	0.782[a]	1,100	3.568	0.49
	40.2[b]	1.290[b]	1,100	3.568	0.49
	39.50[c]	1.490[c]	1,100	3.568	0.49
6 – Pituitary Gland	59.70[a]	1.040[a]	1,053	3.687	0.51
	58.1[b]	1.500[b]	1,053	3.687	0.51
	57.70[c]	1.700[c]	1,053	3,687	0,51
7 – Spinal Cord	32.50[a]	0.574[a]	1,075	3.630	0.51
	30.9[b]	0.843[b]	1,075	3.630	0.51
	30.50[c]	0.951[c]	1,075	3.630	0.51
8 – Muscle	55.00[a]	0.943[a]	1,090	3.421	0.49
	53.5[b]	1.340[b]	1,090	3.421	0.49
	53,20	1.510	1,090	3,421	0,49
9 – Eyes*	49.60[a]	0.994[a]	1,052	3.615	0.53
	46.3[b]	1.369[b]	1,052	3.100	0.50
	47.88[c]	1.530[c]	1,052	3.043	0.50
10 – Skin	41.40[a]	0.867[a]	1,109	3.391	0.37
	38.9[b]	1.180[b]	1,109	3.391	0.37
	38.40[c]	1.310[c]	1,109	3.391	0.37
11 – Tongue	55.30[a]	0.936[a]	1,090	3.421	0.49
	53.6[b]	1.370[b]	1,090	3.421	0.49
	53.10[c]	1.560[c]	1,090	3.421	0.49
12 – Teeth	12.50[a]	0.143[a]	2,180	1.255	0.59
	11.8[b]	0.275[b]	2,180	1.255	0.59
	11.60[c]	0.328[c]	2,180	1.255	0.59

***values are the same for all frequencies.**

ε_r – permittivity, σ – electric conductivity, ρ – density

[a] – value at frequency of 900 Hz

[b] – value at frequency of 1,800 Hz

[c] – value at frequency of 2,100 Hz

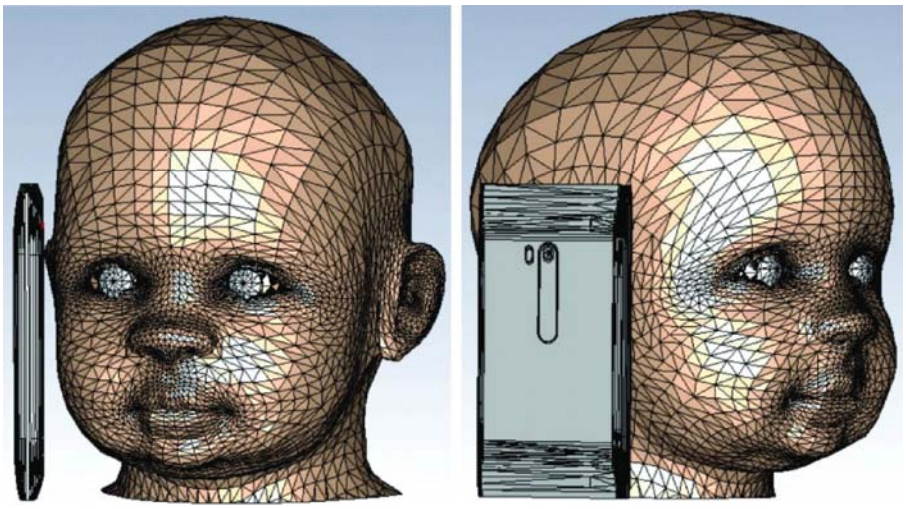

Fig. 1 – External look of the child's head model.

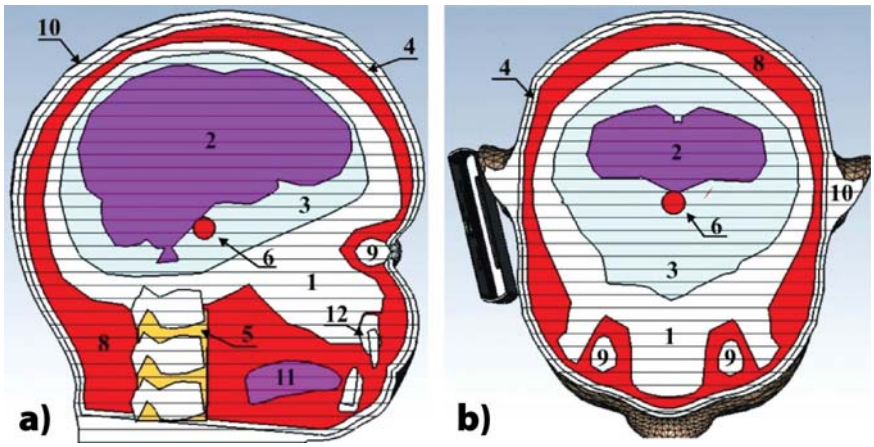

Fig. 2 – a) Vertical and b) Horizontal cross-section of the child's head model. 1 – cortical bones, 2 – brain, 3 – cerebrospinal fluid, 4 – fat, 5 – cartilage, 6 - pituitary gland, 8 – muscle, 9 – eyes, 10 – skin, 11 – tongue, 12 – teeth (the numbers are the same as in Table 1).

In this study actual smartphone (Figure 1) was used as a source of electromagnetic radiation. The mobile phone consisted of following parts: planar inverted F antenna (PIFA), display and mobile housing. The planar inverted F antenna (PIFA) as a source of electromagnetic radiation was modeled for three different frequencies: 900 MHz, 1,800 MHz, and 2,100 MHz, with reference power of $P = 1$W [13] and impedance of $Z = 50\ \Omega$.

The numerical calculation was performed for open space (reflected electromagnetic waves and the other sources of electromagnetic radiation were not taken into consideration). The only source of electromagnetic radiation in this simulation was a mobile phone with an output power of 1W, defined according to the Standard of the Institute of Electrical and Electronics Engineers (IEEE) C.95.3 [13].

Results

The penetration depth of the electric field was the largest in the case of the electric field at a frequency of 900 MHz (Figure 3a). On the other hand, the penetration depth of the electric field at the higher frequencies was smaller resulting in a stronger electric field in tissues that are close to the source of electromagnetic radiation such as mobile phone (Figures 3b and 3c). The peak of the electric field in the pituitary gland at the frequency of 2,100 MHz was less than those at the frequencies of 1,800 MHz and 900 MHz (0.3045 V/m, 0.8643 V/m, and 5.6615 V/m, respectively) (Figure 4).

SAR values averaged over 1 g and 10 g of the tissue for all three frequencies used in this study are presented in Figures 5 and 6, respectively.

Because the penetration depth of electric field was the largest in case of the frequency of 900 MHz (Figure 6), SAR values in the region of the pituitary gland was the highest for this frequency and amounted SAR1g = 0.08521 W/kg (Figure 5) and SAR10g = 0.10325 W/kg (Figure 6).

Discussion

In this study, the electric field distribution within the child`s head model was investigated for different frequencies

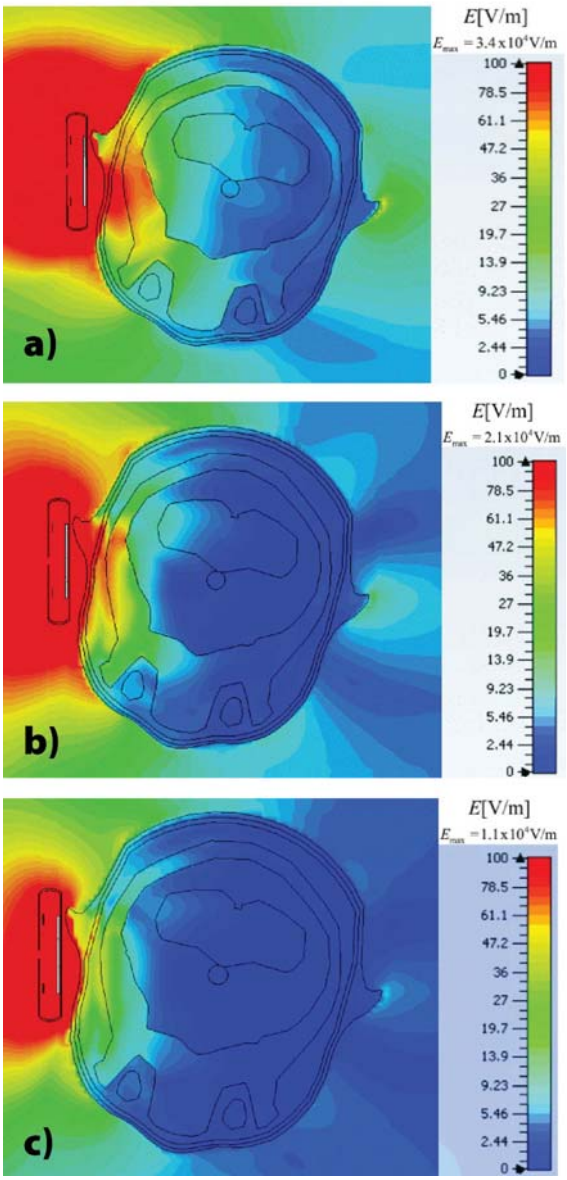

Fig. 3 – Electric field distribution within the child's head model for frequency of a) 900 MHz, b) 1,800 MHz, and c) 2,100 MHz.

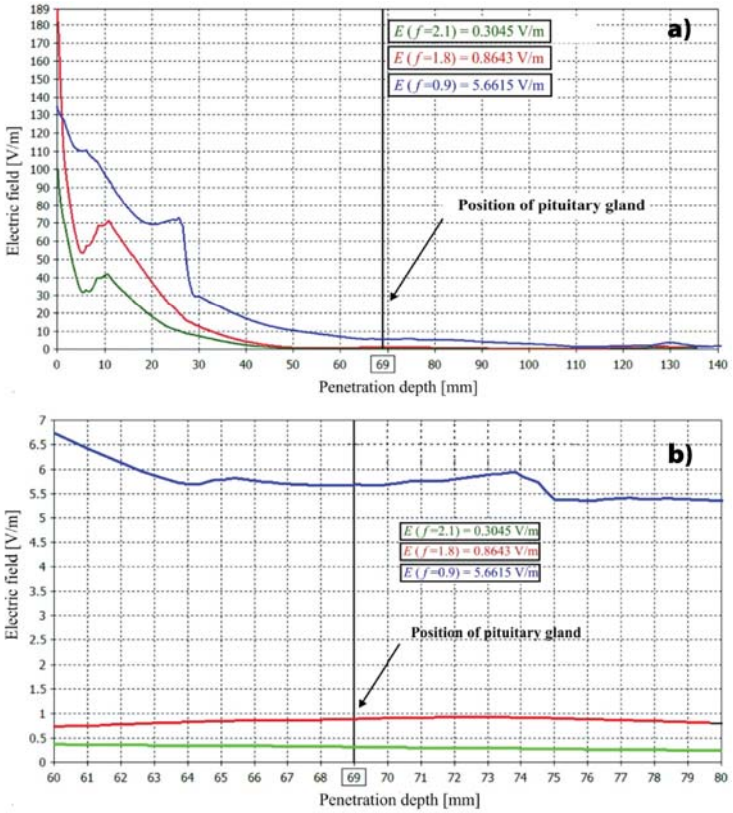

Fig. 4 – Penetration depth of electric field through the child's head model for three different frequencies (f). a) from 0 mm to 140 mm; b) from 60 mm to 80 mm.

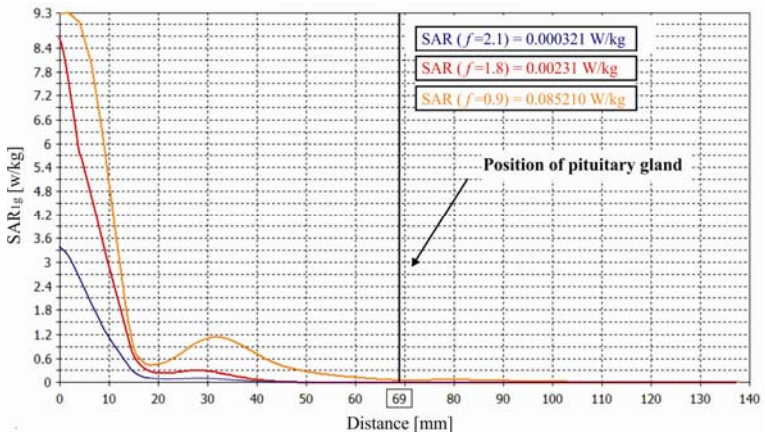

Fig. 5 – Comparative analysis of specific absorption rate (SAR_{1g}) for different frequencies (f) through the child's head model.

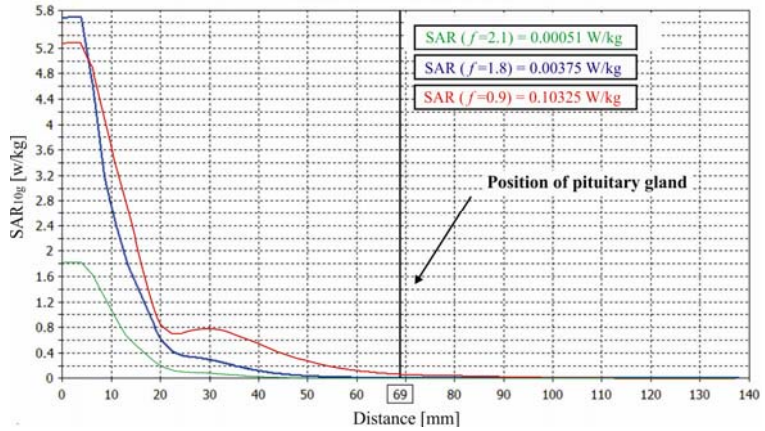

Fig. 6 – Comparative analysis of specific absorption rate (SAR_{10g}) for different frequencies (f) through the child's head model.

of a mobile phone. Our results showed that the penetration depth of the electric field was the largest at a frequency of 900 MHz and decreased at higher frequencies resulting in a stronger electric field in tissue that was close to the source of electromagnetic radiation like a mobile phone. The wavelength of electromagnetic waves has an impact on penetration depth because it varies for different frequencies and it has to be taken into consideration that electromagnetic properties are different for different biological tissues [14].

Generally, the one part of the energy due to the propagation of electromagnetic waves penetrates into certain biological object and it is being absorbed. Differences of wave energy at the boundaries of a biological object (the input energy and output energy) represent the absorbed energy. Because of the need to precisely introduce this absorbed energy it was defined as the term Specific Absorption Rate - SAR. The values of the SAR are different for different tissues and electromagnetic waves of different characteristics, in this case, different frequencies. It can be said that SAR characterizes the interaction of electromagnetic fields with biological tissue. SAR is related to a certain point as an extremely small area in a biological tissue in which the electromagnetic field can be considered as homogeneous one. More practical value is the average SAR as the ratio of the absorbed power in the body and the body mass of biological entity.

For this research, values for the average SAR over 10 g and 1 g of tissue were calculated. Because of different frequencies values of SAR varied. Accordingly, the penetration depth of the electric field was the largest in case of a frequency of 900 MHz, and SAR values in the region of the pituitary gland were the highest for this frequency

The results obtained in this paper are compared with those obtained in the study of Krstić et al. [15]. After comparison, it can be concluded that the value of SAR in the region of pituitary gland for child`s head model used in this research, is greater than SAR in a model of adult person`s head with few layers in that study [15]. SAR in a case of child`s head model is almost five times greater than results in a case of adult`s head model. This is expected due to different characteristics of the model: size, different thickness of layers and therefore the pituitary gland was at greater distances from the source in case of adult person`s head model.

There are many differences among different countries in Europe in terms of upper limits for RF radiation from GSM mobile telephony. Based on Recommendation 1999/519/EC, the limit values which are prescribed for the electric field strength for the following frequencies: 900 MHz, 1,800 MHz, and 2,100 MHz, are 41 V/m, 58 V/m i 61 V/m, respectively[16]. The certain European governments have adopted lower values such as for example Greece (32 V/m, 45 V/m and 47 V/m), Belgium (21 V/m, 29 V/m and 31 V/m), Serbia (16.5 V/m, 23.3 V/m and 24.4 V/m), Slovenia (13 V/m, 18 V/m and 19 V/m), Poland (7 V/m, 7 V/m and 7 V/m), Italy (6 V/m, 6 V/m and 6 V/m), Switzerland (4 V/m, 6 V/m and 6 V/m), etc. for all three frequencies, respectively [17].

The values for the maximum field strength that are prescribed by the standard are given for free space in the absence of people. We have to keep in mind that the values for field strength inside the biological tissues or organs are lower because of the propagation through the material environment and due to the increasing distance from the radiation source.

If the value of the field is known inside biological tissue then, based on the boundary conditions at the surface of the two separate areas, the value of the incident field can be evaluated. Since the value of the electric field in the pituitary gland is known, based on the relationship that is valid for the normal vector components of the electric field at the separate area, the value of the field before the penetration of EM waves in the pituitary gland can be determined.

Based on the value of the dielectric constant and conductivity of air and pituitary gland for different frequencies, the ratio of electric fields strengths at the separate surface of these two areas can be approximately determined. This is certainly the worst case, from the standpoint of the electric field strength, because in this case it does not take into consideration the impact of other layers on the weakening of electromagnetic wave that spreads from the radiation source. However, this approach can give us information about the minimum field strength to which man is exposed, and if it is greater than allowed.

The ratio of normal vector components of electric field at the crossover semiconductor environment is determined from the expression

$$\frac{\underline{E}_1}{\underline{E}_2} = \frac{\sigma_2 + j\omega\varepsilon_2}{\sigma_1 + j\omega\varepsilon_1} \quad (2)$$

For different frequencies and the corresponding values for the dielectric constant and conductivity of the air and the pituitary gland, the ratio of the normal components of the electric field for these two environments is calculated by using previously formula (2) and results are:

$$\left|\underline{E}_{\text{air}} / \underline{E}_{\text{p. gland}}\right\|_{f=0.9\text{GHz}} \approx 63 \text{ V/m},$$

$$\left|\underline{E}_{\text{air}} / \underline{E}_{\text{p. gland}}\right\|_{f=1.8\text{GHz}} \approx 60 \text{ V/m, and}$$

$$\left|\underline{E}_{\text{air}} / \underline{E}_{\text{p. gland}}\right\|_{f=2.1\text{GHz}} \approx 59.5 \text{ V/m.}$$

Based on the previously obtained values for the electric field strength in the pituitary gland, the values of the electric field strength in the air are:

$$\underline{E}_{\text{air}}\big|_{f=0.9\text{GHz}} \approx 356.67\,\text{V/m}$$

$$\underline{E}_{\text{air}}\big|_{f=1.8\text{GHz}} \approx 51.86\,\text{V/m} \text{ , and}$$

$$\underline{E}_{\text{air}}\big|_{f=2.1\text{GHz}} \approx 18.12\,\text{V/m} .$$

If we compare this value with the maximum permissible values specified in the above mentioned countries, we can conclude that they are considerably higher or in range with the maximum allowable ones. Of course, if we take into account the impact of all other layers between the radiation source and pituitary gland obtained values would have been far greater.

Pituitary gland as one of the most important glands of the endocrine system, *via* ACTH has an impact on the cortex

of the adrenal gland. In this way, it stimulates the secretion of steroid hormones.

Some investigations revealed that stimulation of the adrenal axis by electromagnetic radiation from a mobile phone in rats has as a consequence general hyperthermia. In animals exposed to high levels of electric fields, stimulation of the hypothalamic-hypophysial-adrenocortical (HHA) axis was found, mediated by the central nervous system (CNS) [18].

Another very important function of the pituitary gland is that it secretes gonadotropins FSH and LH that regulate testicular spermatogenesis and steroidogenesis. The impact of a mobile phone radiation on gonadotropins level has been considered in man and animals. The results of some studies have shown that a mobile phone radiation cannot cause significant biological effects. But there is a possibility that the time of exposure to radiation from a mobile phone in these studies was not long enough to show some significant biological effects [19–20].

Research conducted by Fang et al. [19] showed progressive histological derangement in rat pituitary glands. These derangements were manifested in the form of swollen mitochondria as well as dilatation of Golgi complex and diffusive lysosomes. Also, this research revealed that with increasing duration of exposure and electromagnetic wave energy this disorder increased. For instance, it has been observed also and mitochondrial vacuolization, the formation of myelin figures, distinct dilatation of endoplasmic reticulum, the occurrence of numerous secondary lysosomes, and clustering of heterochromatin under the nuclear membranes[19].

In the study of Eskander et al. [21], it was shown that people living a long period of time in the vicinity of base stations have a significant reduction of the release into the blood of a number of hormones, including ACTH which is produced and secreted by the anterior pituitary gland [21]. The highly significant decrease of serum cortisol levels in people exposed to electromagnetic radiation was also found.

Conclusion

The penetration depth of the electric field is the largest at the frequencies of 900 MHz and decreases, at the higher frequencies, resulting in a stronger electric field in the tissues that are close to the source of electromagnetic radiation (mobile phone).

Results obtained by numerical analysis show that the electric field at the frequency of 900 MHz has the greatest impact on the pituitary gland, which is a consequence of the highest penetration depth as mentioned before.

This level of radiation may cause substantial harmful health effect in children having in mind our study results that the level of electric field strength inside pituitary gland is higher than the values for the maximum field strength specified by the standard.

R E F E R E N C E S

1. *Foster KR, Chou CK.* Are Children More Exposed to Radio Frequency Energy From Mobile Phones Than Adults. IEEE Access 2014; 2: 1497−509.
2. *Gandhi OP.* Yes the Children Are More Exposed to Radiofrequency Energy From Mobile Telephones Than Adults. IEEE Access 2015; 3: 985−8.
3. *Khalatbari WG, Sardari D, Mirzaee AA, Sadafi HA.* Calculating SAR in two models of the human head exposed to mobile phones radiations at 900 and 1800 MHz. PIERS Online 2006; 2(1): 104−9.
4. *World Health Organization.* Classifies Radiofrequency Electromagnetic Fields as Possibly Carcinogenic to Humans. France, Lyon: IARC; 2011. Available from: http://www.iarc.fr/en/mediacentre/pr/2011/pdfs/pr208_E.pdf
5. Regulation of the limits of exposure to non-ionizing radiation. "Official Gazette of the Republic of Serbia", No. 36/09.
6. *Djeridane Y, Touitou Y, Seze R.* Influence of electromagnetic fields emitted by GSM-900 cellular telephones on the circadian patterns of gonadal, adrenal and pituitary hormones in men. Radiat Res 2008; 169(3): 337−43.
7. *Stanković V, Jovanović D, Ilie S, Marković V.* Electric Field Distribution in Human Head. Timisoara, Romania: CEMEMC; 2014.
8. *Stanković V, Jovanović D, Krstić D, Cvetković N.* Electric Field Distribution and SAR in Human Head from Mobile Phones. The 9th International Symposium on Advanced Topics in Electrical Engineering; Bucharest; 2015 May 7-9. Washington, DC: IEEE; 2015.
9. *Peyman A, Gabriel C.* Dielectric properties of tissues. Moscow, Russia: WHO Workshop on Dosymetry of RF Fields 2005.
10. 3ds Max. Available from: http://usa.autodesk.com/
11. COMSOL. Design and develop better products, faster. Available from: http://www.comsol.com
12. *Clemens M, Weiland T.* Discrete Electromagnetism With The Finite Integration Technique. PIER 2001; 32: 65−87.
13. IEEE Standards. C95.3-2002 - IEEE Recommended Practice for Measurements and Computations of Radio Frequency Electromagnetic Fields With Respect to Human Exposure to Such Fields, 100 kHz-300 GHz.
14. *Stanković V, Jovanović D, Krstić D, Cvetković N, Marković V.* Thermal Effects on Human Head from Mobile Phones. 12 International Conference on Telecommunications in Modern Satellite, Cable and Broadcasting Services (TELSIKS); Niš, Serbia; 2015 October 14−17; Abstract. Washington, DC: IEEE 2015; p. 205−8.
15. *Krstić D, Zigar D, Petković D, Sokolović D, Dinđić B, Cvetković N,* et al. Predicting the biological effects of mobile phone radiation absorbed energy linked to the MRI-obtained structure. Arh Hig Rada Toksikol 2013; 64(1): 159−68.
16. Council Recommendation of 12 July 1999 on the Limitation of Exposure of the General Public to Electromagnetic Fields (0 Hz to 300 GHz). Official Journal of the European Communities 199(59); 1999.
17. *Stam R.* Comparison of international policies on electromagnetic fields (power frequency and radiofrequency fields Bilthoven, Netherlands: National Institute for Public Health and the Environment; 2011. [cited 2014 Jun 11]. Available from: http://ec.europa.eu/health/electromagnetic_fields/docs/emf_comparison_polices_en.pdf.
18. *Black DR, Heynick LN.* Radiofrequency (RF) effects on blood cells, cardiac, endocrine, and immunological functions. Bioelectromagnetics 2003; Suppl 6: S187−95.

19. *Fang HH, Zeng GY, Nie Q, Kang JB, Ren DQ, Zhou JX,* et al. Effects on structure and secretion of pituitary gland in rats after electromagnetic pulse exposure. Zhonghua Yi Xue Za Zhi 2010; 90(45): 3231−4. (Chinese)
20. *Hamada AJ, Singh A, Agarwal A.* Cell Phones and their Impact on Male Fertility: Fact or Fiction. Open Reprod Sci J 2011; 5: 125−37.
21. *Eskander EF, Estefan SF, Abd-Rabou AA.* How does long term exposure to base stations and mobile phones affect human hormone profiles? Clin Biochem 2012; 45(1−2): 157−61.

Received on November 30, 2015.
Revised on January 18, 2016.
Accepted on February 10, 2016.
Online First October, 2016.